

REPORT DOCUMENTATION PAGE			Form Approved OMB NO. 0704-0188	
<small>Public reporting burden for this collection of information is estimated to average 1 hour per response, including the time for reviewing instructions, searching existing data sources, gathering and maintaining the data needed, and completing and reviewing the collection of information. Send comment regarding this burden estimate or any other aspect of this collection of information, including suggestions for reducing this burden, to Washington Headquarters Services, Directorate for Information Operations and Reports, 1215 Jefferson Davis Highway, Suite 1204, Arlington, VA 22202-4302, and to the Office of Management and Budget, Paperwork Reduction Project (0704-0188), Washington, DC 20503.</small>				
1. AGENCY USE ONLY (Leave blank)		2. REPORT DATE 30 June, 2000		3. REPORT TYPE AND DATES COVERED Final Report: 1 Oct. 1999 to 31 Mar. 2000
4. TITLE AND SUBTITLE Selective Photon Light Pipe Experiments			5. FUNDING NUMBERS DAAD19-99-C-0049	
6. AUTHOR(S) K. C. Chen, Daniel J. Krommenhoek, Pedro Sarmiento (Quantum); Ray Beach, Steve Payne Luis Zapata (LLNL); John Myer (Kigre, Inc.)				
7. PERFORMING ORGANIZATION NAME(S) AND ADDRESS(ES) Quantum Group, Inc. 11211 Sorrento Valley Road San Diego, CA 92121			8. PERFORMING ORGANIZATION REPORT NUMBER	
9. SPONSORING / MONITORING AGENCY NAME(S) AND ADDRESS(ES) U.S. Army Research Office P.O. Box 12211 Research Triangle Park, NC 27709-2211			10. SPONSORING / MONITORING AGENCY REPORT NUMBER ARO 40461.1-RT	
11. SUPPLEMENTARY NOTES The views, opinions and/or findings contained in this report are those of the author(s) and should not be construed as an official Department of the Army position, policy or decision, unless so designated by other documentation.				
12a. DISTRIBUTION / AVAILABILITY STATEMENT Approved for public release; distribution unlimited.			12b. DISTRIBUTION CODE	
13. ABSTRACT (Maximum 200 words) Report developed under SBIR contract. A feasibility study of using a combustion-driven light source to pump a 1540 nm eye-safe phosphate glass fiber laser was performed. The proposed laser pumping concept consists of a 980 nm narrow-band ytterbia selective emitter and a transparent sapphire filament light pipe that transfers the light to an eye-safe erbium-doped ytterbium phosphate fiber laser. The maximum radiant exitance and irradiance of the selective emitter light pipes (SELP) were analyzed and experimentally determined. The maximum irradiance with ytterbia SELP, to date, is at 9.7 W/cm ² with 32.4 mW power output measured on a 425µm sapphire light pipe. The ytterbia SELP is currently below the pumping irradiance threshold of 11 (optimistic) to 35 W/cm ² for the phosphate glass double-clad fiber laser. A new double-clad two stage fiber laser pumped by neodymium SELP was identified as an alternative design.				
14. SUBJECT TERMS SBIR Report, Eye-safe, Laser, Selective Emitter, Light Pipe, Rare-Earth Oxide, Ytterbia, Combustion			15. NUMBER OF PAGES 30	
			16. PRICE CODE	
17. SECURITY CLASSIFICATION OR REPORT UNCLASSIFIED	18. SECURITY CLASSIFICATION OF THIS PAGE UNCLASSIFIED	19. SECURITY CLASSIFICATION OF ABSTRACT UNCLASSIFIED	20. LIMITATION OF ABSTRACT UL	

NSN 7540-01-280-5500

Enclosure 1

Standard Form 298 (Rev. 2-89)
Prescribed by ANSI Std. Z39-18
298-102

20001122 147

Selective Light Pipe Experiments

Contract No. DAAD19-99-C-0049

Prime Contractor

K. C. Chen, Dan Krommenhoek and Pedro Sarmiento
Quantum Group, Inc.
11211 Sorrento Valley Road
San Diego, CA 92121

Subcontractors

Ray Beach, Steve Payne and Luis Zapata
Lawrence Livermore National Laboratory
P.O. Box 808, L-482
Livermore, California 94550

and

John D. Myers
Kigre, Inc.
100 Marshland Road
Hilton Head, SC 29926

Sponsored by

U.S. Army Research Office
P.O. Box 11211
Research Triangle Park, NC 27709-2211

The views and conclusions contained in this documentation are those of the authors and should not be interpreted as representing the official policies, either expressed or implied, of the U. S. Army Research Office or any part of the U. S. Government

Table of Contents

LIST OF FIGURES	iii
LIST OF TABLES	iv
1. STATE OF THE PROBLEM STUDIED	2
2. SUMMARY OF THE MOST IMPORTANT RESULTS	3
3. MAJOR AREA OF EFFORT	4
3.1 ANALYSES AND SIMULATION	4
3.1.1. <i>Radiant Exitance of Ytterbia Selective Emitter</i>	4
3.1.2. <i>Light Pipe Material</i>	6
3.1.3. <i>SELP Light Transmission Simulation</i>	6
3.1.4 <i>SELP Fiber Laser Design</i>	9
a. <i>The Laser</i>	9
b. <i>Architectural Considerations</i>	10
3.1.5. <i>Feasibility Study of SELP in Pumping Laser Fiber</i>	11
a. <i>Super Emissive Light Pipe</i>	12
b. <i>Er,Yb:Phosphate Glass Fiber Laser</i>	14
3.2. SELP CONFIGURATION AND EXPERIMENTS	18
4. CONCLUSION	24
5. SUGGESTION FOR FUTURE WORK	24
5.1 HIGH-TEMPERATURE OPTICAL MATERIAL IMPROVEMENTS	25
5.2 FIBER LASER COMPOSITION AND CONFIGURATION IMPROVEMENTS	25
6. BIBLIOGRAPHY	26

List of Figures

Figure 1.	Phase diagram of Al_2O_3 - Yb_2O_3 . The arrow indicates the composition of ytterbia-sapphire SELP is close to alumina end.....	6
Figure 2.	Hypothetical blackbody (bb) and SELP in contact with the same thermal reservoir to bring them into thermal equilibrium.....	12
Figure 3.	Black body spectrum of 2134 C emitter.....	14
Figure 4.	Example of laser energetic calculation in which developed laser power is plotted against pump input irradiance.....	15
Figure 5.	Er:Yb phosphate glass fiber laser model used for calculation.....	15
Figure 6.	Energetic plot for various values of fiber loss, Er concentration, and ambient temperature.....	16
Figure 7.	SELP experiments to determine the effect of side-coating.....	20
Figure 8.	Side-coated multiple section SELP experiments with three MAPP torches.....	20
Figure 9.	The schematic and results of multiple torch SELP experiments. Runs 6 and 8 show absorption occurs in side-coatings.....	21
Figure 10.	SELP experiments on single crystal sapphire filament reach a maximum of $5\text{-}6 \text{ W/cm}^2$	22
Figure 11.	Experiments with ytterbia emitters detached from light pipes.....	23
Figure 12.	Test setup using small torch and ytterbia felt.....	23
Figure 13.	Emission spectrum taken at the end of sapphire light pipe using ytterbia felt as the emitter source.....	24
Figure 14.	Double core eye-safe laser pumping design. SELP first pumps a Nd-doped core, which, in turn, pumps Er:Yb eye-safe fiber laser.....	26

List of Tables

Table 1. Spectral exitance of ytterbia between 2000 and 3500°K.....5

Table 2. Selective emitter light pipe simulations on side coating effect.....8

Table 3. Three selective emitters on light pipe.....9

Table 4. The simulation input parameters and output results for
SELV-pumped fiber laser.....17

1. State of the Problem Studied

An efficient Er:glass laser operating at an eye-safe wavelength near 1.54 μm will expand many applications such as rangefinder, laser radar, communication, security systems, and atmospheric data measurements. These "eye-safe" lasers require the lasing wavelength outside the visible range allowing the energy to exceed 79 micro-joules only in a 0.02 μm -wide bandwidth center at 1.54 μm in the infrared range.

An eye-safe laser rod contains erbium and ytterbium ions, the erbium ion is the light-emitting dopant and ytterbium or chromium are sensitizer ions. An eye-safe laser phosphate glass, for example, contains 15-22 weight percent of ytterbium ($1 \times 10^{21}/\text{cm}^3$) and is doped with 0.26 weight percent of erbium ($1.2 \times 10^{19}/\text{cm}^3$). The sensitizing ions play an important role in the pumping process. Since the concentration of Er is typically low, it is insufficient to pump the Er ions directly as the absorption is weak. The concentration of the sensitizing ytterbium ions can be considerably greater and can capture the excitation efficiently, then transfer the energy to erbium ions to produce a population inversion and lasing action [1].

The most common laser excitation source for eye-safe lasers is a flashlamp or light-emitting diodes. Due to the broad emission spectrum in the flashlamp, flashlamp-pumped erbium glass lasers are limited to relatively low repetition rates due to the need of dissipating excess heat. The low repetition rate precludes erbium glass to be used in eye-safe radar applications.

A new light source, ytterbia (Yb_2O_3)-coated light pipe, offers the new opportunity for efficiently pumping an eye-safe laser with a combustion heat source. When heated to incandescence, ytterbia emits a narrow 980nm band matching perfectly with the long-wavelength edge of the broad Yb^{3+} absorption in the Er/Yb phosphate. There is minimal out-of-band infrared spectrum that greatly reduces the excess heat in the laser glass. The passive light pipe made of high temperature transparent material, such as single crystal sapphire, transfers the light directly to the laser rod. This combination of rare-earth emitter and light pipe is termed selective emitter light pipe (SELP). As with laser diode pumping at 980 nm, the SELP light source is also inherently efficient and induces low thermal loading to the glass and should result in a more stable output and higher repetition rates for eye-safe radar applications.

Success with the SELP pumping scheme, however, relies on the prerequisite of SELP reaching the laser threshold brightness and with adequate pump energy. Experiments are performed to determine the irradiance versus emitter surface area relation. Additional experiments are intended to maximize the irradiance while preserving the lifetime of the SELP. Quantum Group's task is to provide the highest irradiance achievable from SELP.

The laser-pumping brightness threshold, pump energy, and corresponding laser power output are calculated by the subcontractor team at Lawrence Livermore National Laboratories (LLNL) by varying various laser rod parameters, including the doping levels and laser rod design. The fiber laser rod design is provided by Kigre, Inc. The challenge is to find the minimum irradiance threshold and pump power in a laser design that can produce an efficient laser output. Three teams interact to determine the feasibility of a proof-of-concept laser configuration.

Through these data, the feasibility of using readily available portable combustion sources to drive an eye-safe laser system can be evaluated. The successful application of SELP will eventually bring portability to laser systems based on alternative energy sources.

2. Summary of the Most Important Results

We first determine the theoretical spectral exitances of ytterbia between 2000-3500°K. At its melting temperature (2623°K), the spectral exitance of ytterbia is 25.5 W/cm^2 based on integrating the blackbody curve between $1.0 \pm 0.1 \mu\text{m}$, and assuming a constant emissivity of 0.7. This value is the thermodynamic limit of ytterbia for laser pumping in air. When the light enters a material with refraction index of n , the maximum irradiance can be boosted by a factor of n^2 . Therefore, the directional in-band emissive power in a materials with refractive index of 1.5 (refractive index of laser phosphate glass) is $18.3 \cos(\theta) \text{ W/cm}^2\text{-sr. } (25.5/\pi \times 1.5^2)$.

The light pipe experiments were first carried out in fused silica SELP with MAPP/air torch as heat source. The irradiance was in the range of 0.5 W/cm^2 to 1 W/cm^2 in fused silica SELP. The relation between incandescent emitter surface area and irradiance at the end of the light pipe was examined. The results indicated irradiance soon saturates with only moderate increase in side coating surface area. The ray tracing simulation on light pipe shows that the side coating is less efficient than the end coating in transferring the emitted light to the end. Self-absorption in the side-coating may contribute to the saturation and lower than expected irradiance at the end of SELP.

From the phase diagrams of ytterbia-alumina binary system, ytterbia-coated sapphire SELP has operational temperature limit at the melting temperature of sapphire, 2050°C (2323°K). To operate SELP at ytterbia's melting temperature, the ytterbia emitter was then detached from light pipe. Methane and oxygen were used to increase the flame temperature and a small torch tip was used to focus the flame to a very small area. Different emitter light pipe configurations were tested. The irradiance improved to 5 W/cm^2 and then to 9.7 W/cm^2 . At the present time, a power output of 13.5 mW was obtained on a 425 μm diameter sapphire filament. Higher values may be possible by using better collecting optics and single crystal zirconia as the light pipe. Scalability in power output was demonstrated by using three filaments. A higher power output of 32.4 mW was obtained. The irradiance, however, decreases to 7.7 W/cm^2 that may be due to a less favorable light collecting geometry at the end of the SELP.

With the maximum radiant exitance and experimental irradiance roughly defined, the pumping requirements for eye-safe phosphate glass laser were then calculated using a core-cladding fiber laser rod design. This unique core-cladding laser rod design provided by Kigre Inc. traps the pumping light by total refraction along the laser rod axis allowing them to be completely absorbed by the core. The goal of simulation is to lower the irradiance threshold and pump power requirements by adjusting laser rod parameters, including the fiber laser length, cladding geometry, core and cladding area ratio, erbium and ytterbium concentrations, temperature and passive loss in the phosphate glass. For the first iteration, the calculation indicates the pump irradiance threshold is around 35 W/cm^2 and the required pump power is 200 mW for a 200 μm diameter fiber laser. The phosphate glass contains $1 \times 10^{19}/\text{cm}^3$ of Er^{3+} ions and $3 \times 10^{21}/\text{cm}^3$ of

Yb³⁺ ion. The pump irradiance threshold can be as low as ~11 W/cm², if Er concentration is reduced to 1x10¹⁸/cm³, very low loss of 1dB/km, at -77°C and sacrificing the laser efficiency.

From these studies, a factor of 3 (optimistic) to 5 increase in pump irradiance is needed for pumping the current fiber laser design. It is possible to increase the SELP radiance since it is below the theoretical limit of 25.5 W/cm². The follow-on research is to modify the fiber laser design to bring down the pump irradiance requirement even further. It is suggested that SELP can be used first to pump a Nd laser, which, in turns, can pump the Er eye-safe laser. The operating temperature of the ytterbia emitter can be increased above 2400°C by forming solid solution with zirconia or hafnia. This will increase the radiant exitance of the emitter.

Preliminary evaluation performed after the completion of this contract indicates feasibility of SELP pumping lasers. This improvements includes new geometry, optical parameters and materials. New Kigre laser pumping concept, and LLNL evaluation for these improvements will be reported in the follow-on contract report.

3. Major Area of Effort

3.1 Analyses and Simulation

3.1.1. Radiant Exitance of Ytterbia Selective Emitter

The generation of light by thermal radiators is governed by Plank's radiation law, which the spectral energy distribution of a blackbody is described by:

$$E_0(\lambda, T) = \frac{c_1 \lambda^{-5}}{\exp(c_2 / \lambda T) - 1} \quad (1)$$

with two constants $C_1 = 2hc^2 = 1.19 \times 10^{-16} \text{ W/m}^2$
 $C_2 = hc/k = 1.438 \times 10^{-2} \text{ m } ^\circ\text{K}$

(h is Plank's constant, c is the velocity of light, and k is Boltzmann's constant).

The energy distribution of an non-ideal radiating body can be written as:

$$E = \epsilon E_0 \quad (2)$$

The factor ϵ , the emissivity, depends in general on the wavelength λ , the temperature T and the angle Θ at which the energy is radiated.

The second principle-Kirchhoff's radiation law relates the emissivity of the radiating body to its absorption:

$$\epsilon(\lambda, T, \Theta) = A(\lambda, T, \Theta) \quad (3)$$

where A is the absorption factor of the radiating body. The maximum radiant exitance of any

material in incandescence is described by the Plank's blackbody curve, which, by definition, has an invariant emissivity of 1 at all wavelengths. In section 3.1.5, LLNL provides analyses that demonstrate that the spectral emissive power of the selective emitter will not be higher than a blackbody at the same temperature.

To obtain the maximum *spectral* emittance of the selective emitter at various temperatures, the areas under the blackbody curves in the narrow-bandwidth ($1 \pm 0.1 \mu\text{m}$) of the selective emitter were calculated. These values are then adjusted with the assumption that ytterbia has a constant emissivity value of 0.7 and a constant 200 nm bandwidth emission at these temperatures [2] (Note: In section 3.1.5, LLNL used a conservative bandwidth of 100 nm for simulation). Table 1 lists the spectral emittance of ytterbia between 2000 to 3500°K. The theoretical spectral exitance of ytterbia in vacuum at its melting temperature 2623°K is 25.5 W/cm^2 .

Since ytterbia is a Lambertian light source, the in-band radiance is then $8.1 \text{ W/cm}^2\text{-steradian}$ ($25.5/\pi$) in air. When the light enters a material with refraction index of n , the maximum irradiance can be boosted by a factor of n^2 . Therefore, the directional in-band emissive power in a materials with refractive index of 1.53 (refractive index of laser phosphate glass) is $19.0 \cos(\theta) \text{ W/cm}^2\text{-sr}$ (8.1×1.53^2).

Several flame temperatures including methane, propane, MAPP gas with air and oxygen as oxidizers are given to show the maximum spectral exitance possible for each fuel (Table 1).

Table 1 Spectral exitance of ytterbia between 2000 to 3500°K.

Temp. T (°K)	Blackbody $M_{\lambda\text{max}}(T)$ ($\text{W/cm}^2\text{-}\mu$)	Line Emitter (@ $1 \mu\text{m}$) W/cm^2	Ytterbia Spectral Exitance @ 0.9- 1.1 μm and $\epsilon = 0.7$ W/cm^2	Spectral Exitance for fused silica $n^2 = 1.5^2$ concentration	Flame Temperatures and Materials Limitations
2000	41.168	28.1	3.94	8.87	
2100	52.542	39.6	5.55	12.49	$T_{\text{flame}}^{\text{Methane/air}} = 2153^\circ\text{K}$
2200	66.302	54.1	7.58	17.06	$T_{\text{mp}}^{\text{Yb}_3\text{Al}_5\text{O}_{12}} = 2213^\circ\text{K}$ $T_{\text{flame}}^{\text{propane/air}} = 2240^\circ\text{K}$
2300	82.804	72.0	10.07	22.66	$T_{\text{mp}}^{\text{Al}_2\text{O}_3} = 2326^\circ\text{K}$
2400	102.439	93.4	13.08	29.43	$T_{\text{flame}}^{\text{MAPP/air}} = 2366^\circ\text{K}$
2500	125.635	118.8	16.63	37.42	
2600	152.854	148.4	20.78	46.76	
2700	184.599	182.3	25.52	57.42	$T_{\text{mp}}^{\text{Yb}_2\text{O}_3} = 2673^\circ\text{K}$
2800	221.411	220.8	30.91	69.55	
2900	263.876	263.9	36.95	83.14	
3000	312.619	311.7	43.64	98.19	

3.1.2. Light Pipe Material

Light pipe materials are selected for their high temperature stability, low emissivity in the near infrared region, high optical transmission characteristics, and available geometry. The sapphire melts at 2050°C and has low spectral emissivity at 1 μ m [2]. When constructing selective emitter light pipe, possible high-temperature solid-state reactions should be considered. Figure 1 shows the phase diagrams of Al_2O_3 - Yb_2O_3 . The ytterbium aluminate garnet ($\text{Yb}_3\text{Al}_5\text{O}_{12}$) melts at 1900°C. The methane/air flame temperature is 1880°C (2153°K). The ytterbium aluminate garnet interacts with alumina and forms eutectic liquid at 1750°C. With MAPP flame temperature at 2093°C (2366°K), for example, ytterbia coating on alumina rod will eventually form a melt. The melting temperature of ytterbia is reported to be at 2350-2400°C.

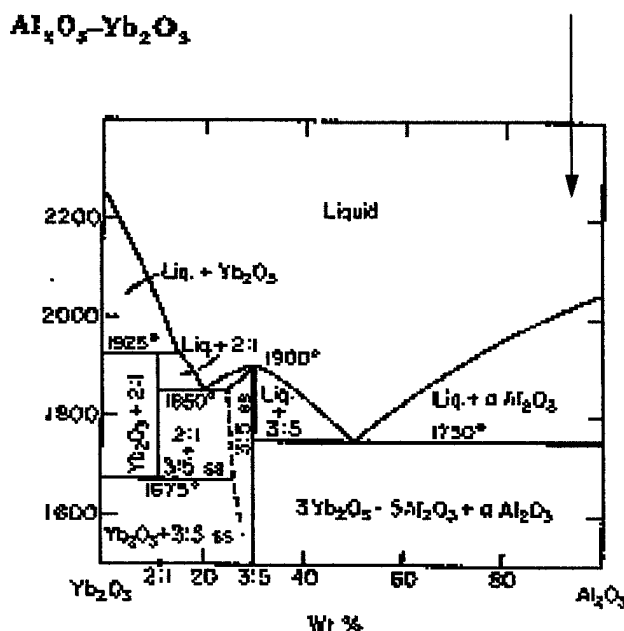


Figure 1 Phase diagram of Al_2O_3 - Yb_2O_3 . The arrow indicates the composition of ytterbia-sapphire SELP is close to alumina end [4].

The arrow in the figure indicates the average composition of ytterbia-alumina light pipe system. The ytterbia-sapphire light pipe forms liquid slightly below sapphire's melting temperature.

From the phase diagrams, only separation of ytterbia from alumina can prevent high temperature eutectic reactions, thus allowing the ytterbia to be used close to its melting temperature. To be used close to the melting temperature, the only limitation will be imposed by the evaporation rate of ytterbia. It has been reported that ytterbia has an equilibrium partial pressure $\approx 10^{-6}$ of the molecular YbO at 2300°K [5].

As will be described in the section 3.2, the initial SELP experiments were performed on ytterbia emitter attached to light pipes. The latter experiments were done with detached ytterbia. This allows us to obtain much higher irradiance.

3.1.3. SELP Light Transmission Simulation

Optical evaluation of the SELP was obtained with geometric optic analysis software. We were able to calculate the irradiance and radiance for a wide range of selective emitter and light pipe parameters. The design of an efficient selective emitter light pipe to pump a laser requires balancing the tradeoff between providing irradiance uniformity, maximizing the collection efficiency from the source and minimizing the size of the optical package. The calculations were performed through use of Optical Research Associates LightTools illumination software Version 2.1. This illumination analysis software uses a non-sequential ray trace method that follows the laws of optics and represents physical reality for mechanical structures where they are absorbed, reflected or scattered. Generally >100,000 rays are traced for each simulation.

Table 2 summarizes selective emitter light pipe calculations for fused silica and sapphire light pipes. Selective emitter coatings are simulated by emitting and absorbing coatings applied to either (or both) the end and sides of these light pipes. The selective emitter coating source is set at a source surface exitance of 14.1 watts/cm^2 . Thus, end and side coating power and length are set to give this surface exitance. The inner material refractive index for the first three groups is characteristic of fused silica, for the fourth group of sapphire, while the outer refractive index is characteristic of a ytterbia selective emitter.

This table shows simulations for four selective emitter portraits. The first group of simulations represents a single heated selective emitter source at the end and unheated selective emitter coatings of various lengths along the length of the light pipe. As the length of unheated selective emitter is increased, more photons from the end source are absorbed and the target irradiance decreases from a high value of 9.3 watts/cm^2 to zero at a selective emitter length of 100mm.

The second group represents heated side sources of varying lengths. In general the target irradiance is low compared to the irradiance obtained with an end source.

The third group represents both heated end and side sources. With a heated selective emitter side source with a long length, this absorbs the photons from the heated end source and gives very low irradiance. However, a short side source will not absorb photons from the end source and results in a significantly higher irradiance (by an order of magnitude).

For the fourth group, the inner index is 1.78 that is sapphire. It has a beneficial effect in that the photons from the heated side coatings now stay in the light pipe and do not significantly absorb. This change in inner pipe refractive index results in irradiance increases by a factor of ten.

Table 3 summarizes a simulation where three separate selective emitter coatings are applied to the light pipe. This shows excellent agreement with data. The selective emitter side coatings nearest to the target are most effective in delivering photons to the target. Side coatings absorb photons originating at a distance from the target as they travel down the light pipe.

Simulations have indicated the importance of geometry and refractive index. Significantly larger target irradiance is possible with a unique geometry that has selective emitter rectangular light pipes bonded to square high index light gathering waveguides. This will be recommended for future work.

Table 2. Selective emitter light pipe simulations on side coating effect

INNER RADIUS mm	OUTER RADIUS mm	INNER INDEX	OUTER INDEX	END SOURCE Power watts	SIDE SOURCE Power watts	SIDE SOURCE Length mm	SIDE SOURCE Absorb or Reflect	TARGET Irradiance watts/cm ²
End Coating Only - Side Absorber Length Variations								
1.45	1.50	1.5	1.8	1	0	0	TIR	9.3
		1.5	1.8	1	0	0.1	Absorb	5.1
		1.5	1.8	1	0	1	Absorb	4.3
		1.5	1.8	1	0	10	Absorb	0.3
		1.5	1.8	1	0	100	Absorb	0
Side Source Only - Length Variation								
		1.5	1.8	0	130	100	Absorb	0.2
		1.5	1.8	0	13	10	Absorb	0.2
		1.5	1.8	0	1.3	1	Absorb	0.3
Combined End and Side Source								
		1.5	1.8	1	130	100	Absorb	0.2
		1.5	1.8	1	13	10	Absorb	0.4
		1.5	1.8	1	1.3	1	Absorb	4.6
Higher Inner Index - Sapphire (1.8) vs. fused silica (1.5)								
		1.78	1.8	1	0	100	Absorb	0
		1.78	1.8	0	130	100	Absorb	5.0
		1.78	1.8	1	130	100	Absorb	4.9
		1.78	1.8	0	13	10	Absorb	4.3
		1.78	1.8	0	1.3	1	Absorb	1.9

All source irradiance = 14.1 watts/cm²

Light pipe: length=200 mm

Outer: radius=1.50 mm

Inner: radius=1.45 mm



End source Side source with range of coating lengths

All sources emit and may absorb other incident photons

Irradiance at target with
side source only coated
on light pipe
1.3 watt - 1 mm long

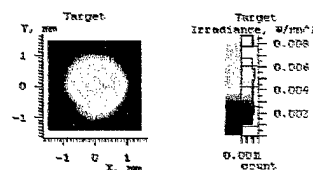
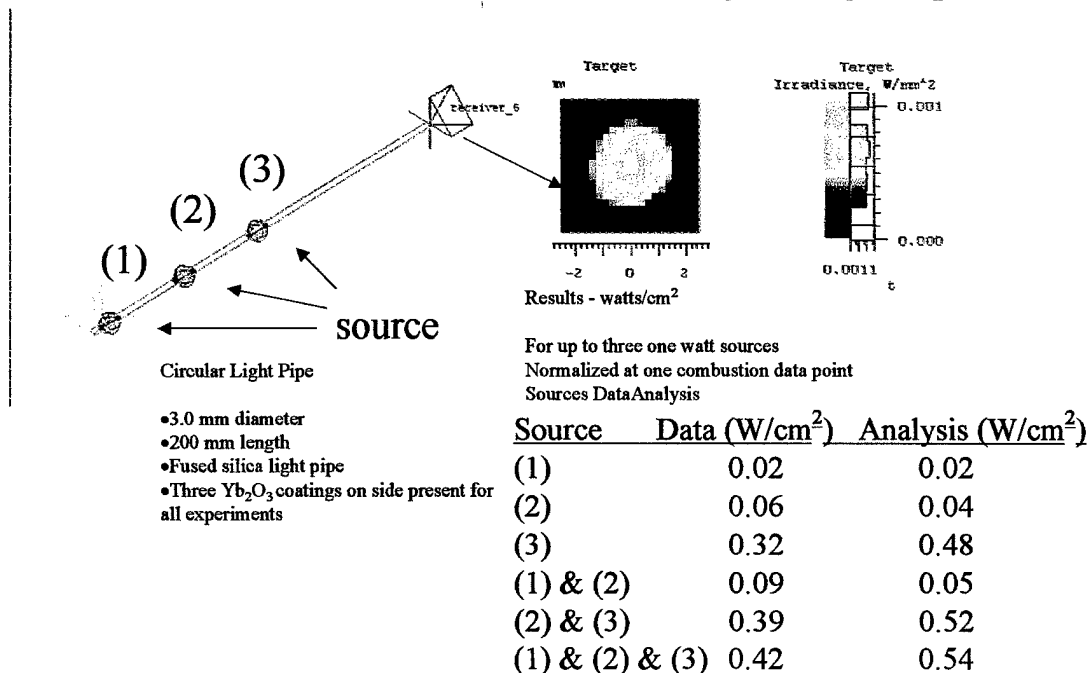


Table 3. Three Selective Emitter Coatings on Light Pipe



3.1.4 SELP Fiber Laser Design

(The section is described by John D. Myers of Kigre, Inc.)

In this section we explore a method of adapting the pumping requirement of Er/Yb doped fiber laser architecture to the output characteristics of a super-emissive light pipe (SELP). In this analysis we have relied upon computer simulation by Dr. Ray Reach et. al. of Lawrence Livermore Laboratories as well as upon experimental evidence gleaned at Kigre, Inc. and elsewhere in the laser community. It appears that by combining two double-clad pumping architectures we can accomplish the task of mating the relatively low brightness SELP to the high brightness requirement of the fiber laser without violating any law of thermodynamics.

Early in the discussions concerning the SELP-pumped laser design, it was recognized that mating the relatively low brightness SELP emitter to the lasing element would be a technical challenge in that the lasing element requires significant brightness of its pump radiation just to overcome threshold. Of the many designs considered, the cladding-pumped fiber laser appeared to offer the best chance of success, considering its high efficiency and most important, the relief offered to the pumping radiation brightness due to the large pump NA in relation to the lasing core NA required for single mode operation. Subsequently, the SELP characteristics and the double-clad fiber laser material and structural characteristics were studied and analyzed. The work at Kigre is to concentrate on the cladding pumped laser design.

a. The Laser

Material consideration: The material chosen from which to fabricate the cladding pumped fiber laser is Kigre's QX phosphate laser glass. This material has several properties which, relative to silica, make it uniquely desirable for this application, requiring the combination of high gain per unit length plus the flexibility necessary to produce the complicated structures at reasonable cost. A list of these properties relative to silica is shown as follows:

Property	QX	Silica
Emission Cross Section ($\times 10^{-20} \text{ cm}^2$)		
Ytterbium (wavelength in nm)	1.4 (1025-1065)	0.5 (1050-1140)
Erbium (wavelength in nm)	0.8 (1535)	0.3 (1544)
Neodymium (wavelength in nm)	3.8 (1054)	1.4 (1064)
Solubility of Rare Earth (Wt. %)		
Ytterbium	>30	<2.0
Erbium	>20	<0.2
Neodymium	>25	<0.2

The high emission cross sections of the QX phosphate glasses plus their high levels of solubility (relative to their silica counterpart) can be combined to provide levels of gain per unit length of 3-5 dB/cm versus the silica fiber norms of approximately 1 dB/meter. Therefore, one can expect equivalent fiber laser operation in QX glass in shorter lengths than in silica, by two orders of magnitude.

Note: Kigre, Inc. demonstrated greater than 25 dB gain in an 8 centimeter section and 10 dB gain in a 2 centimeter section of Er/Yb doped QX phosphate glass single mode fiber earlier this year. This performance is now considered standard in these types of fibers. Cladding pumped versions of these fibers are considered the best candidates for this application

b. Architectural Considerations:

After one makes the assumption to operate single mode at a given wavelength, the remaining design criteria involving doping levels, fiber lengths, core/cladding ratios, numerical apertures, and the like can then be extrapolated from existing experimental data and further evaluated by computer simulation. The general relationships between these parameters are described as follows:

Doping levels: In a fiber laser, one wishes to reach saturated gain levels as rapidly as possible for maximum efficiency. Therefore, we need complete inversion over the entire core length. In the erbium/ytterbium system, the physical disposition of the pump power is determined by the Ytterbium doping. The gain per unit length and the inversion level is determined by the number of Erbium ions per unit length relative to the available pump power per unit length. Therefore, we determine the ytterbium dopant level necessary to distribute the pump energy uniformly

along the core. We then determine the maximum erbium dopant level for which we have sufficient power to maintain complete inversion. From experimental data, we can approximate these levels to a degree sufficient for prototyping and computer simulation studies.

Core/Cladding ratios: For a given doping level, the ratio of core area to cladding area in a cladding pumped fiber laser determines the length over which the pump radiation is absorbed by the core. For example, in a ytterbium fiber laser doped at 1.5 Wt.% with a core to cladding area ratio of 1 to 1000, it took 50 meters of fiber length to absorb 90% of the pump radiation into the core. The length of fiber required to absorb the pump radiation is inversely proportional to the ratio of core to cladding areas. In the same manner, as one would expect, for a given core to cladding area ratio, the length required to absorb 90% of the pump radiation is directly proportional to the doping level of the core.

Active Ion: Both the erbium and ytterbium systems are quasi-three level systems which have an absorption cross section (threshold) which must be overcome before one can enter the gain region. Neodymium, however, is a four level system with no absorption cross section and thus, a very low threshold made up only of small background losses at the lasing wavelength (1054 nm). As a result, neodymium lasers have much more lower threshold (1/10) for lasing and are thus more attractive when faced with low brightness pump sources.

Computer Simulations: Based upon the above considerations, computer simulations by Dr. Ray Beach at Lawrence Livermore Laboratories have run with the following results:

1. A 200 cm long, Er/Yb fiber laser yields an output of less than 1 milli-watt at 1535 nm at input of approximately 40 Watts per square centimeter. (The detailed description of simulation result is given in the following section (3.1.5))
2. A 50 cm long Nd fiber laser yields an output of approximately 33 milli-watts at 1054 nm at precisely the same power.

The question naturally arises, "Can we pump the Er/Yb fiber laser with the output of the Nd laser?" The answer is resounding, "Yes". The simulation will be performed and documented in the follow-on program.

3.1.5. Feasibility Study of SELP in Pumping Laser Fiber

(The following analyses were performed by Dr. Ray Beach, Dr. Luis Zapata and Dr. Steve Payne of Lawrence Livermore National Laboratory. Please note these calculations were based on a maximum usage temperature of 2134°C, 0.1 μm bandwidth, and a lower irradiance measurement, 5 W/cm² in air, obtained in the beginning of the program)

The feasibility of using a so-called super-emissive light pipe (SELP) to pump a Er,Yb-codoped phosphate glass fiber was explored. In order to accomplish this, we need to first understand the level of brightness that is attainable from a SELP, and then determine whether the Er,Yb: fiber can reach threshold. Having framed the problem in this way, this paper is to be regarded as a plausibility study.

a. Super Emissive Light Pipe

SELP technology is currently reduced to practice by affixing rare earth (RE) emitters to a sapphire fiber (using RE compounds), which are normally emissive at their resonant frequencies. The question arises as to what the maximum attainable emission rate of the SELP can be. It turns out that the achievable brightness [$\text{W}/(\text{cm}^2 \text{nm})$] is necessarily always less than or equal to that of a blackbody, even if there is a narrow emission line characterizing the light output.

Consider a blackbody with unity absorption over the entire spectrum, and a SELP with unity absorption over a very narrow spectral range, $\lambda_1 < \lambda < \lambda_2$, and zero absorption everywhere else. This is a somewhat simplified view of a SELP, as the absorption can in general range between zero and one, but here the simplified model serves to make our point. Imagine both the blackbody and the SELP are brought to the same temperature by contacting them with a thermal reservoir at temperature T . Further, imagine the blackbody and SELP are coupled together with a perfectly reflecting tube allowing them to exchange thermal radiation. See Fig. 2 below.

The following qualitative argument shows that the SELP spectrum cannot have a higher spectral brightness than the blackbody spectrum in its region of emission, $\lambda_1 < \lambda < \lambda_2$. This proposition will be proven by *reductio ad absurdum*. Assume the spectral brightness of the SELP in its region of emission exceeds the spectral brightness of the blackbody when both are at the same temperature T . On removing the two bodies from the thermal reservoir so that they form an isolated system, the blackbody will then spontaneously heat and the SELP will spontaneously cool. This of course is a contradiction to the second law of thermodynamics, as we would have a situation in which the entropy of a closed system (SELP plus blackbody) decreased. Therefore the original assumption must be wrong, and so the spectral brightness of the SELP must be less than or equal to the spectral brightness of the blackbody in the SELP's region of emission.



Figure 2: Hypothetical blackbody (bb) and SELP in contact with the same thermal reservoir to bring them into thermal equilibrium.

This situation can be presented somewhat more quantitatively as follows. The population ratio in a collection of two-level atoms can be described at any instant by an "atomic temperature" T_a

$$N_2 / N_1 = \exp(-h\nu / k T_a) \quad (4)$$

At the same time, the ratio of spontaneous and noise-stimulated emission rates, to noise-

stimulated absorption rates, is related to the temperature T_{rad} of the electromagnetic surroundings by

$$(W_{21} + \gamma) / W_{12} = \exp (h\nu / k T_{rad}) \quad (5)$$

where W_{21} is noise-stimulated emission rate, γ is the spontaneous emission rate and W_{12} is noise-stimulated absorption rates. The ratio of energy flow rates in the two directions is thus given by

$$Power\ out\ of\ atoms / Power\ into\ atoms = \exp [(h\nu / kT_{rad}) - (h\nu / kT_a)] \quad (6)$$

These rates will be equal and opposite if and only if the atomic temperature T_a exactly equals the surrounding electromagnetic temperature T_{rad} . So the net energy received by the atoms from the blackbody fields will exactly equal the energy radiated back to the surroundings by the atoms.

Overall thermal equilibrium requires that the blackbody absorption and spontaneous emission rates be in exact equilibrium, transition by transition for each of the multilevel atoms. This necessity for the net absorption and spontaneous emission to be in balance on each individual transition at thermal equilibrium is sometimes referred to as "*detailed balance*". It applies not only transition by transition, but also frequency component by frequency component, irrespective of line shape.

Having shown that the SELP can at most match the brightness of a black body emitter, we take the temperature of the system to be $T = 2134^\circ\text{C}$, the maximum feasible value that can be envisaged (coated sapphire SELP). The curve is show below in **Figure 3**, where we can assign the region near 0.88 to 0.98 μm to the region useful for pumping the Yb^{3+} ion. Reading from the chart we are able to see that the total spectral emittance is $80\text{ W}/(\text{cm}^2\text{-}\mu\text{m})$. Assuming that the source is Lambertian, the angular distribution that gives rise to the emittance in **Fig. 3** is:

$$I(\theta) = \frac{80}{\pi} \frac{W}{\text{cm}^2 \mu\text{m sr}} (0.1 \mu\text{m}) n^2 \cos(\theta) = 2.54 n^2 \cos(\theta) \frac{W}{\text{cm}^2 \text{sr}} \quad (7)$$

where θ is defined relative to the surface normal and n is the refractive index that is being radiated into. When considering the use of a SELP to pump a fiber laser, proper consideration has to be given to the numerical aperture (NA) of the fiber structure that is to contain and transport the pump light down the length of the fiber. Here we consider a pump confining structure with a NA of 0.4, which is typical of what can be achieved using a double clad fiber structures. A NA of 0.4 corresponds to θ varying between 0° and the $\sin^{-1}(0.4)=23.6^\circ$. So, the total irradiance useful for pumping the fiber is given by the following integral of the angular distribution given in eq. (7) over solid angle,

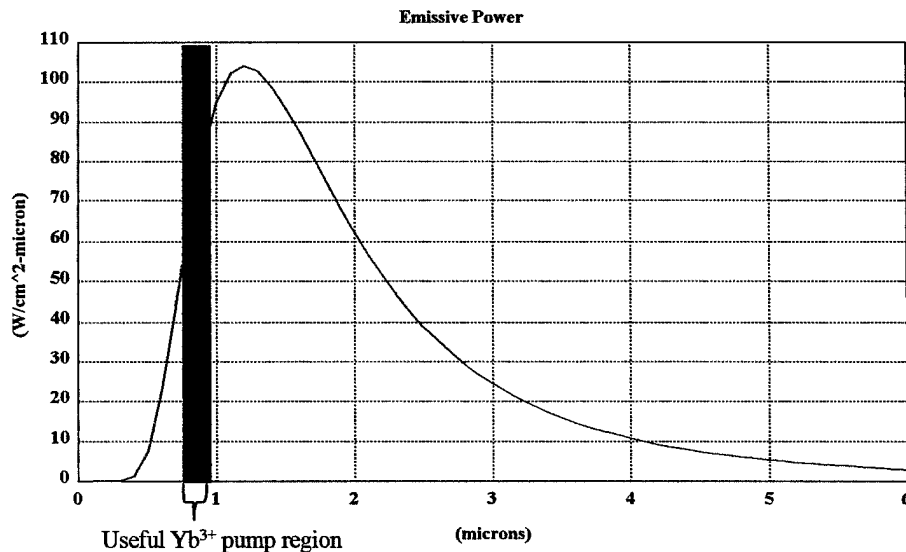
$$I_{\text{useful for fiber}} = \int_0^{2\pi} d\phi \int_0^{23.6^\circ} d\theta \sin(\theta) I(\theta) = 2.9\text{ W} / \text{cm}^2 \quad (8)$$

Double-ended pumping would in principle lead to an available pump irradiance of $5.8\text{ W}/\text{cm}^2$.

Black body spectrum at 2134 C into vacuum



- Total blackbody emissive power into vacuum:



- Directional emissive power into useful pump spectral region with index n:

$$\frac{1}{\pi} 80 \frac{W}{cm^2 - \mu m} (0.1 \mu m) n^2 \cos(\theta) \approx 2.54 n^2 \cos(\theta) \frac{W}{cm^2 - sr}$$

Figure 3: Black body spectrum of 2134°C emitter.

b. Er,Yb:Phosphate Glass Fiber Laser

The model of the Er,Yb:phosphate glass requires consideration of the Yb^{3+} to Er^{3+} energy transfer (K) and the Er^{3+} Auger upconversion (c), as noted in the kinetic equations below (Figure 4). In addition, the Yb^{3+} absorption and emission cross sections at the pump wavelength ($\sigma_{a,Yb}$ and $\sigma_{e,Yb}$), Er^{3+} absorption and emission cross sections at the laser wavelength ($\sigma_{a,Er}$ and $\sigma_{e,Er}$), and the emission lifetimes of the excited states (τ_{Er} and τ_{Yb}), must be accounted for where I_p and I_l are the pump and laser irradiances in the fiber, respectively. After deducing the ground and excited state populations of the ions ($n_{2,Yb}$, $n_{2,Er}$ and $n_{1,Er}$), the intra-cavity laser intensity I_l can be determined for a given value of the pump intensity I_p , yielding the predicted laser output power. The schematic of fiber laser model for simulation is shown in Fig. 5. An example of this calculation follows where the pump intensity is plotted against the laser output power (Figure 6) for the case of the parameters noted in the Table below (Table 4).

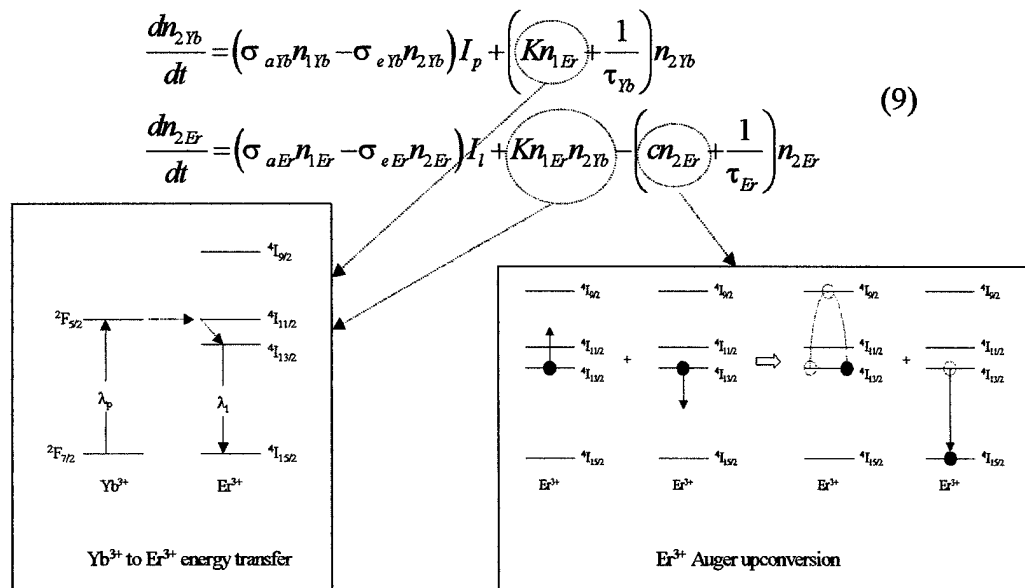
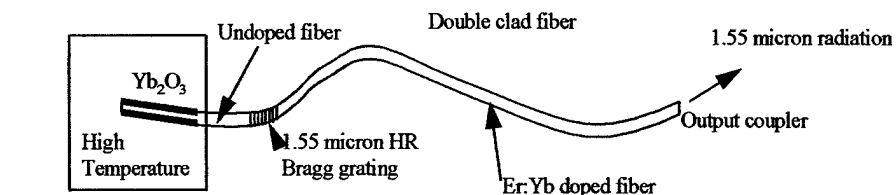


Figure 4: Example of laser energetic calculation in which developed laser power is plotted against pump input irradiance

Er:Yb phosphate glass fiber laser model



• Double clad fiber oscillator conceptual design



• Fiber cross section

1st iteration

Undoped pump cladding
NA~0.4

Er:Yb doped core

2nd iteration based on rectangular
cladding width × height = 300 × 400 μm

10 microns

200 microns

Figure 5: Er:Yb phosphate glass fiber laser model used for calculation

Temperature dependence can also be incorporated into our laser modeling by including the thermal dependence of the populations in the various Yb and Er Stark levels involved with the laser process. By varying the passive fiber loss and the temperature we can gain some insight into the lowest possible threshold believed to be attainable for the Er^{3+} , Yb^{3+} co-doped fiber. In the plot that follows two Er concentrations are investigated, 10^{18} cm^{-3} and 10^{19} cm^{-3} , the other fiber parameters are the same as in the preceding table 4.

Looking at the projected performance in Fig. 6, it is seen that to achieve good slope efficiency the higher Er concentration of 10^{19} cm^{-3} is required. However, even at liquid nitrogen temperatures (-77°C) at this higher Er concentration, a pump irradiance within the capture angle of the fiber cladding structure of greater than 25 W/cm^2 will be required to achieve lasing. The calculated SELP pump irradiance that can be usefully delivered into the fiber is 2.9 W/cm^2 for an emissivity of unity (5.8 W/cm^2 for double-sided pumping), suggesting that this approach faces the challenge of inadequate pump brightness. The case of 1 dB/km loss, an Er concentration of 10^{18} cm^{-3} , and a temperature of -77°C , offers a threshold of 11 W/cm^2 , seemingly close the available pump irradiance of 5.8 W/cm^2 . But in consideration of the level of optimism reflected in these assumptions: very low loss, very low impurity concentration ($\ll 100$ ppm) to accommodate the low Er concentration, need for sub-ambient temperature, and ideal SELP emissivity and collection efficiency -- caution is advised in pursuing the SELP-pumped Er,Yb:phosphate fiber approach.

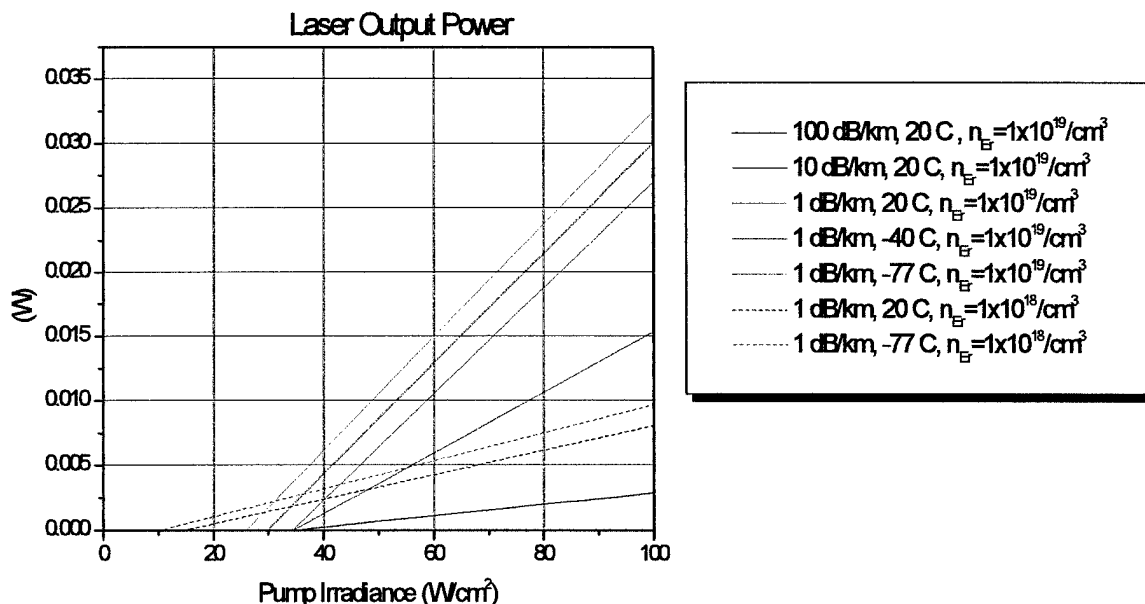


Figure 6. Energetics plot for various values of fiber loss, Er concentration, and ambient temperature.

Table 4. The simulation input parameters and output results for SELP pumped fiber laser.

Input	Name	Output	Comment
200	l_s		length of fiber (cm)
.0005	r_core		radius of Er:Yb doped core (cm)
.03	w_pump		width of pump cladding (cm)
.04	h_pump		height of pump cladding (cm)
	A_core	7.85398E-7	area of Er:Yb doped core (cm ²)
	A_pump	.0012	area of pump cladding (cm ²)
	Vs	.00015708	volume of doped core (cm ³)
.957	eta_l		laser mode overlap with core
	eta_p	.000654498	pump mode overlap with core
	Tpercm	.999997697	waveguide transmission per cm
-.00001	dBpercmT		passive waveguide transmission in dB/cm
	T	.999539589	1-way cavity transmission
.99	Roc		output coupler reflectivity
0	Rp		pump reflectivity after a single pass
1	eta_del		pump delivery efficiency
	eta_abs	.935992257	pump absorption efficiency
	Iout	5238.51692	laser intensity (W/cm ²)
	Pp	.054	pump input power (W)
45	Ip		pump intensity (W/cm ²)
	Ppabs	.050542106	Total absorbed pump power (W)
	Pthermal	.020263721	total thermal power (W)
	Pfl_Er	.014490621	
	Pfl_Yb	.011297511	
	Pfl	.025788133	total fluorescence power (W)
	Plost	.000393891	scattered laser power (W)
	Pcheck	-.00020282	diagnostic, should ~0
1E-18	c		Er Auger constant (cm ³ /sec)
3E-16	K		Yb-Er energy transfer coeff. (cm ³ /sec)
1E19	n0_Er		Er3+ population (1/cm ³)
	n1_Er	5.71037E18	Er3+ 4I15/2 population (1/cm ³)
	n2_Er	4.28963E18	Er3+ 4I13/2 population (1/cm ³)
.006	tau_Er		Er3+ storage lifetime (sec)
	s_a_Er	3E-21	Er3+ 1.55 micron absorption cross section (cm ²)
	s_e_Er	4E-21	Er3+ 1.55 μ emission cross section (cm ²)
1.2903E-19		hvl	laser photon energy (J)
3E21	n0_Yb		Yb3+ population (1/cm ³)
	n1_Yb	2.99944E21	Yb3+ 2F7/2 population (1/cm ³)
	n2_Yb	5.57397E17	Yb3+ 2F5/2 population (1/cm ³)
.001	tau_Yb		Yb3+ storage lifetime
	s_a_Yb	3.5E-21	Yb3+ absorption cross section
	s_e_Yb	4E-22	Yb3+ emission cross section
2.1277E-19	hvp		pump photon energy (J)

3.2. SELP Configuration and Experiments

Fiber laser pumping parameter calculations performed by the LLNL provide the first few iterations on the irradiance required for laser threshold. It should be noted that the calculated irradiance and threshold values, however, vary with fiber laser rod design and dimensions and, therefore, should not be regarded as the final values needed for a successful laser pumping. The goal of further LLNL tasks is to calculate Kigre's fiber laser design to determine the irradiance and threshold requirements. On the other hand, the goal of selective emitter light pipe experiments is to strive for the highest radiant exitance on the ytterbia surface set forth by the thermodynamics limit and materials stability and to obtain highest light collecting efficiency.

There are two methods to coat ytterbia on the light pipes. The first method applies ytterbia coating by brushing a solution containing ytterbia powder suspended in ytterbium nitrate solution. The coating is white and thick (100-250 μ m). The second coating method using a metallorganic liquid. The coating is transparent but thin (0.1-0.3 μ m). Most of the experiments were performed on SELP with thick coating.

The first set of SELP experiment was aimed at increasing irradiance at the end of light pipe as more ytterbia surface area are heated — i.e. more light emitting surface generates more light down the light pipe. Since the experiments are to determine the brightness versus coating surface area increment relation, ytterbia-coated fused silica light pipe ($T_{mp} = 1740^{\circ}\text{C}$) of 3 mm diameter and 20 cm long were used for the experiments. A silicon radiometer sensitive up to 1.1 μ m was used to measure the power. The finely polished distal end of the SELP was pushed against the detector and MAPP/air torches were used to heat the ytterbia coating.

The results are shown in **Figure 7**. The end-coated SELP has irradiance of 0.54 W/cm² (Run 1). In side-coated SELP, the irradiance is 0.31 W/cm² when the flame are able to cover most of the emitter surface at the end (Run 2). The irradiance, however, decreases drastically when a portion of the coating is not heated (Runs 3 and 4). This indicates that the cooler portion of the emitter acts as an absorber. Unlike the end-coated SELP where the light enters the light pipe is confined by total reflection, light refraction occurs into the higher refractive index ($n = 1.8$) ytterbia coating and is absorbed in the side-coated SELP. It implies that for a flame that has a temperature distribution, emitter sections in cooler flame regions will absorb photons emitted from the hotter sections thus averaging the irradiance at the end of the SELP. Therefore, maintaining the same temperature along the length of light pipe is essential to observe the additive effect.

Because of the difficulty in heating the side coating uniformly with point heat sources, like torches, in a long length SELP, multiple emitter sections were applied and torched individually (**Figure 8**). **Figure 9** shows the experiment schematics and results. It shows that the side coatings do not increase the irradiance. Instead, each downstream section absorbs some portion of photons even the sections that are at the same temperature. It can be explained by the fact that, at any instance, a certain fraction of the electrons in ytterbium ion will be at the ground level even at high temperature. These electrons may absorb either photons or excited phonon (from lattice vibration) to a higher energy level. Therefore, some portion of 980 nm light is always absorbed. Since the light transfer efficiency of side coatings is low, as confirmed by

using light tracing software, the additional photons emission by these sections do not fully compensate the absorption loss. From a system point of view, the multiple sections with torches actually lowers the fuel to photon transformation efficiency.

The additive effect is then sought in SELP with shorter coating length, since it is possible to cover the entire surface by two torches (Run 9). There is, however, only a slight increase in irradiance (to 0.55 W/cm^2 or 10% increase). The increase can also be attributed to higher emitter temperature due to higher thermal input. The small increase in irradiance, however, indicates the side coating on the light pipe has a low light transfer efficiency into the light pipe.

Since increasing the surface did not drastically increase SELP irradiance, we then seek to increase radiant exitance of the ytterbia by increasing temperature. It is noticed that there is a flame interference when two closely-spaced torches are aimed at the same location. Irradiance can be lower if two torches are arranged unfavorably. Properly oriented torches increase the irradiance to 0.63 W/cm^2 (Run 9). Drastic irradiance increase can be realized by using a methane/oxygen flame (Run 10). However, the fused silica material limitation is reached—the light pipe bent in a few minutes.

Sapphire filament ($T_{\text{mp}} = 2050^\circ\text{C}$) light pipe was used for SELP higher temperature stability. The $425\mu\text{m}$ diameter sapphire filaments (Saphikon, Inc.) end-coated with ytterbia were used for subsequent experiments. Methane and oxygen gases was used to reach higher flame temperature

Small torches (Smith Equipment 12-1401-06SP and 12-1401-04SP) were used to confine the flame only to the end of the SELP. These torches required low pressure regulators to reduce gas velocity at the torch tip. The fuel input rates were controlled by a rotameter and thermal input was calculated. The results are shown in **Figure 10**. The results show that the irradiance reaches 5 W/cm^2 at sapphire's melting temperature (Runs A25, A27). Higher than 140W of heat input results in melting the sapphire into the sphere and eventually falling off.

In order to reach beyond the sapphire's melting point, we separated ytterbia emitter from the light pipe. Small ytterbia mantles, originally developed for CECOM portable flashlight and TPV power source project, were used as the emitter. The ytterbia mantle is supported by a mullite tube forming a mantle assembly (**Figure 11**, Run 18). The mullite tube was slid onto 3 mm fused silica light pipe. The mini-torch focused the flame only on the mantle thus avoiding reactions between the emitter and light pipe. A 100 mW of power output and 1.4 W/cm^2 irradiance were obtained—roughly three times increase in irradiance observed in fused silica light pipe (cf. Run 1) and a stable SELP structure.

The mantle assembly was then put on the torch side and bare sapphire filament ($\phi 425 \mu\text{m}$) was used as light pipe (**Figure 11**, Run A29). A stable 3-4 mW of power output (2 to 3 W/cm^2 irradiance) can be easily obtained without melting the sapphire filament. With 180 W fuel input rate, a maximum 7.5 mW of power output and 5.4 W/cm^2 irradiance were obtained when the sapphire proximal end is positioned less than 0.5 mm away from the mantle surface. There is a pro and con of using mantle as the emitter source. The pro is that the mantle consists of fine diameter filament which has a very small mass providing rapid thermal equilibrium to the flame temperature and a small thermal gradient. The cons is, at 180 W fuel input rate, the high velocity gas tends to break the mantle if there is a defect.

MAPP/air gas torch (Unless indicated otherwise)
Fused silica light pipe $\phi 3\text{mm}$, $L=200\text{mm}$, ytterbia coating; IL1700 radiometer (200-1100nm)

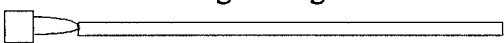

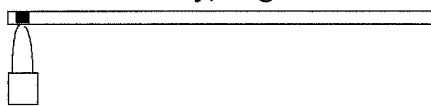
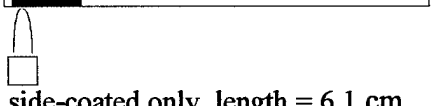
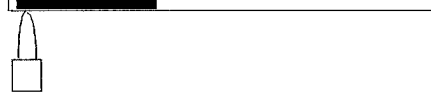
Run #	Schematic	Power Measured	Irradiance
(0)	no coating - background 	0.3 mW	0.00 W/cm ²
(1)	end coated only 	38.1 mW	0.54 W/cm ²
(2)	side-coated only, length = 1.0 cm 	22.0 mW	0.31 W/cm ²
(3)	side-coated only, length = 3.0 cm 	3.5 mW	0.05 W/cm ²
(4)	side-coated only, length = 6.1 cm 	0.8 mW	0.01 W/cm ²

Figure 7. SELP experiments to determine the effect of side coating.

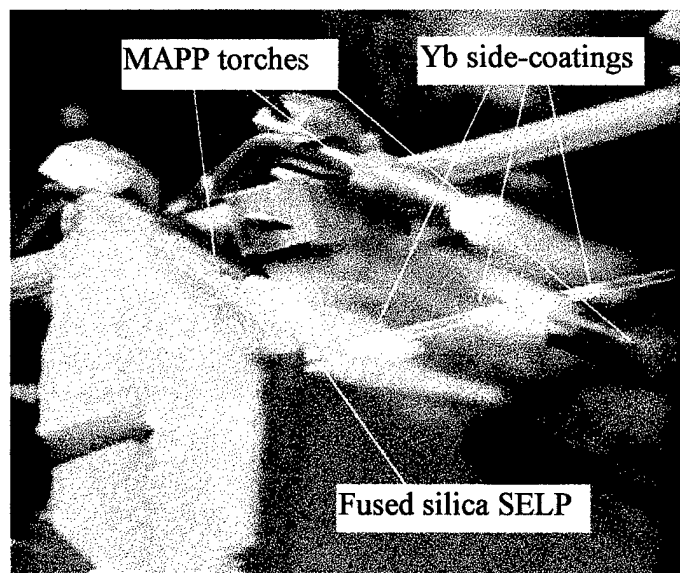
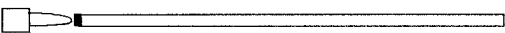

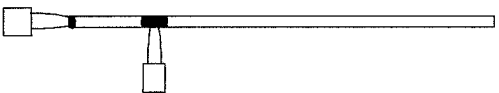


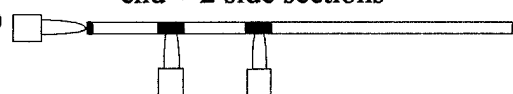

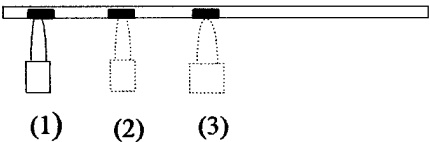
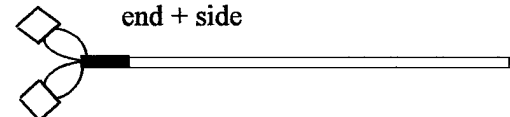
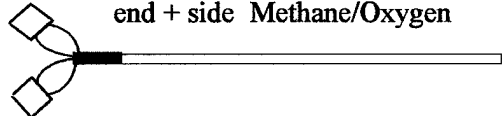


Figure 8. Side-coated multiple section SELP experiment with three MAPP torches.

MAPP/air gas torch, unless indicated otherwise
Fused silica light pipe $\phi 3\text{mm}$, $L=300\text{mm}$, ytterbia coating; IL1700 radiometer (200-1100nm)

Run #	Schematic	Power Measured	Irradiance
(6)	end coating only 	38.1 mW	0.54 W/cm^2
(7)	end + 1 side section 	21.0 mW	0.30 W/cm^2
(7a)	end + 1 side section 	37.0 mW	0.51 W/cm^2
(8)	end + 2 side sections 	9.0 mW	0.13 W/cm^2
(8a)	end + 2 side sections 	16.0 mW	0.23 W/cm^2
(8b)	end + 2 side sections 	38.0 mW	0.54 W/cm^2
(9)	end + side 	39.0 mW	0.55 W/cm^2
(23)	3 side sections 	(1) 1.7 mW (2) 4.2 mW (3) 1.7 mW	0.02 W/cm^2 0.06 W/cm^2 0.02 W/cm^2
(10)	end + side 	45.0 mW	0.63 W/cm^2
(11)	end + side Methane/Oxygen 	90.0 mW* 67.0 mW*	1.27 W/cm^2 0.94 W/cm^2

* Light pipe instability (melt and bend)

Figure 9. Multi-torch SELP experiments. Runs 6 to 8 show absorption occurs in side coatings.

Single crystal sapphire filament ϕ 0.425mm L=280 mm
Methane/Oxygen fuel; mini-torch tips (Smith Equipment #4 and #6)

Run #	Schematic	Power Measured	Irradiance
<p><i>Torch tipsize #6</i></p> <p><i>Fuel Input Rate = 135 W</i></p>			
(A24)		6.7 mW max	4.8 W/cm ²
<p><i>Torch tip size #6</i></p> <p><i>Fuel Input Rate = 155 W</i></p>			
(A25)		7.4 mW max*	5.3 W/cm ²
		* Melt pool grow	
<p><i>Torch tip size #4</i></p> <p><i>Fuel Input Rate = 135 W</i></p>			
(A27)		6.5 mW max [⊕]	4.6 W/cm ²
		[⊕] melt pool stable	
<p><i>Torch tip size #4</i></p> <p><i>Fuel Input Rate = 163 W</i></p>			
(A28)		8.3 mW max [⊙]	5.9 W/cm ²
		[⊙] melt pool unstable	

Figure 10. SELP experiments on sapphire filament reach a maximum of 5-6 W/cm².

To eliminate the weakness of the mantle, a ytterbia felt was used as the light source. Because of the large thermal gradient, the light pipe has to be oriented on the same side as the torch (Figure 12). An improved power output of 9.4-13.5 mW and irradiance of 6.7-9.7 W/cm² were obtained with sapphire light pipe (ϕ 425 μ m) at a distance less than 1 mm away from the felt surface with fuel input rate of 122W. The end of the sapphire filament is a rounded sphere. In order to increase the total power, three sapphire filaments were joined together at the end forming a larger sphere. A higher power output of 32.4 mW was obtained. The irradiance, however, decreases to 7.7 W/cm² because of less favorable light collecting geometry at the end.

Oceanoptics fiber spectrometer was used to confirm the ytterbia spectra at the end of the light pipe. The bandwidth seems to broaden at the end of light pipe (Figure 13).

In summary, a maximum irradiance of 9.7 W/cm² was obtained. It seems possible to further increase the irradiance with a better light collection geometry and higher temperature light pipe materials. We will also test optical quality single crystal ytterbium aluminate garnet and yttrium aluminate garnet SELP to see if a bulk emitter behaves differently than the coating in the continued phase of this program.

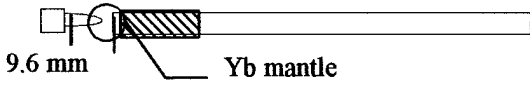
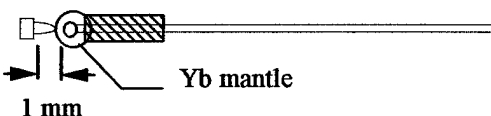
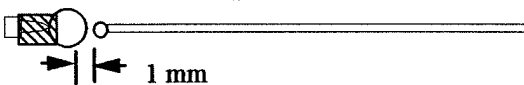
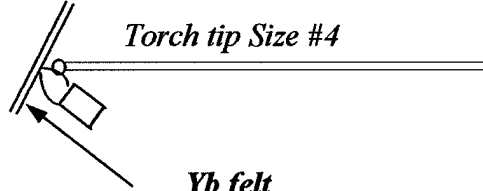
Single crystal sapphire filament ϕ 0.425mm L=280 mm (Unless indicated otherwise) Methane/Oxygen fuel; mini-torch tip (Smith Equipment #6)			
Run#	Schematic	Power Measured	Irradiance
<p><i>Fused Silica, ϕ3mm, Torch tip size #6</i></p> <p><i>Fuel input Rate = 176 W</i></p>			
(18)		100 mW	1.4 W/cm ²
<p><i>Torch tip size #6</i></p> <p><i>Fuel Input Rate = 194 W</i></p>			
(A29)		2.5 mW max	1.8 W/cm ²
<p><i>Torch tip size #4</i></p> <p><i>Fuel Input Rate = 184 W</i></p>			
(A30)		4.1 mW max	2.9 W/cm ²
<p><i>Torch tip Size #4</i></p> <p><i>Fuel Input Rate = 122 W</i></p>			
(A31)		11.3 mW max	9.3 W/cm ²

Figure 11. Experiments with the ytterbia emitters detached from light pipes.

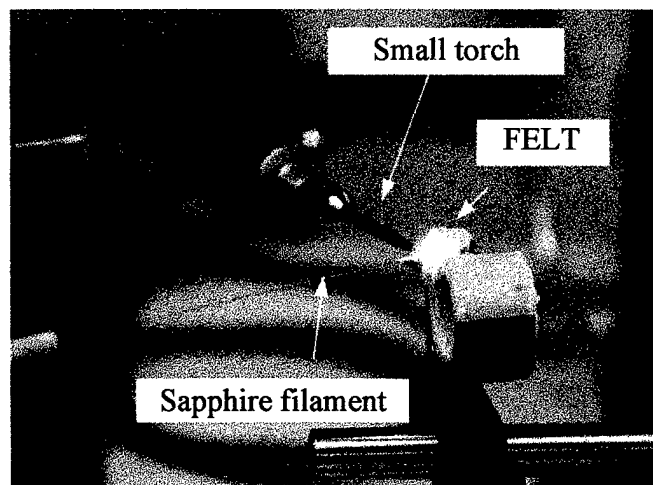


Figure 12. Test setup using small torch and ytterbia felt.

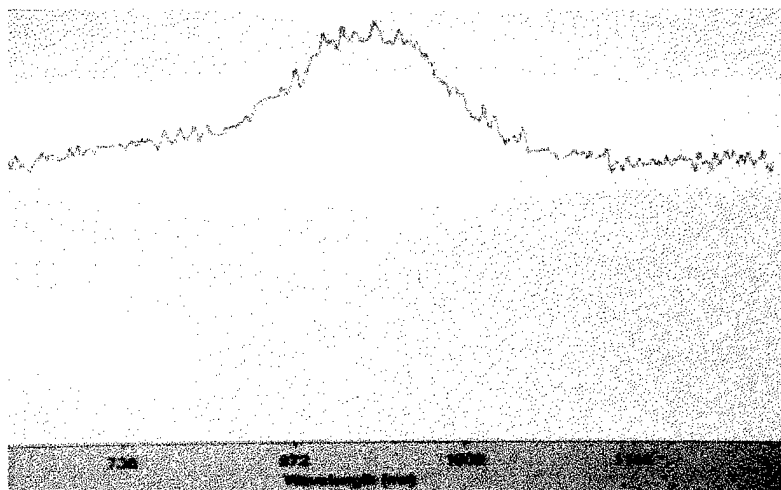


Figure 13. Emission spectrum taken at the end of sapphire light pipe using ytterbia felt as the emitter source.

4. Conclusion

The feasibility of pumping an eye-safe Er:Yb phosphate glass laser through a combustion-driven ytterbia light pipe was examined. To pump an eye-safe laser, the irradiance of the selective emitter light pipe has to deliver an irradiance higher than the lasing threshold.

Initially, the ytterbia light pipes are made of ytterbia coating on either fused silica rods or single crystal sapphire filaments. Increasing in side coating area did not significantly increase in irradiance at the end of light pipe. The melting of sapphire limits the operational temperature to 2050°C. By detaching ytterbia from light pipe, a maximum irradiance of 9.7 W/cm² was achieved close to 2400°C. Further increase in irradiance may be achieved by better light collecting in the light pipe and by increasing the operating temperature above 2400 °C through zirconia incorporation .

An end-pumping clad-core fiber laser configuration was used for laser modeling. The laser threshold was calculated by varying several key parameters, including erbium and ytterbium ions concentration, the core and cladding diameter, and Er and Yb ions absorption cross-sections and laser fiber length. The preliminary result indicates the laser threshold is around 35 W/cm². By sacrificing laser output efficiency and using more optimistic parameters for calculation, the threshold is lower to >15 W/cm².

To close the gap in irradiance and pumping threshold, a new double-cladding laser rod design was proposed. A neodymium light pipe will be used to pump a Nd core-cladding laser which, in turns, pumps another core-cladding erbium ytterbium eye-safe laser. This promising work is in a follow on contract, and will be documented in that follow-on report.

5. Suggestion for Future Work

The near term work for the next months will be focused on increasing selective emitter radiance, improving the photon collecting efficiency and adjusting fiber laser design configuration to lower the laser threshold brightness and pump power requirement.

5.1 High-Temperature Optical Material Improvements

Specifically, the near term focus will be in the following areas:

1. Additional experiments on ytterbia mantles and felt detached from the light pipes with enhanced optical coupling at the end of the light pipe to increase the irradiance. Determine the optimum orientation of light pipe configuration
2. Perform experiments with high quality optical grade single crystal ytterbium aluminum garnet (YbAG) bonded to yttrium aluminum garnet (YAG). The experiments, which will be operated at lower temperature, can provide a better quality light pipe and should enhance coupling from the selective emitter to the light pipe due to high quality optical bond.
3. Construct a combustion furnace which interior is covered with ytterbia emitter. Determine the irradiance of light pipe versus its length in the oven. This configuration should not have the absorption as in the ytterbia-coated SELP.
4. Perform pre- and post-experiment optical analyses of light pipe systems to determine the optical parameters (refractive index, emissivity and absorption coefficient). Since the experiments are performed at up to 2600°K and optical properties of rare-earth oxides do not exist at these temperatures, agreement of analyses with experiments will yield information on the range of optical properties at elevated temperatures, and then provide capability for subsequent selective emitter light pipe experiments.

5.2 Fiber Laser Composition and Configuration Improvements

Several issues in SELP to pump eye-safe lasers are:

1. Evaluate the tradeoffs on laser efficiency and laser threshold irradiance for the expected range of pump irradiance possible with current SELP geometry by modeling.
2. Refine the fiber clad-core laser configuration that provides a better optical coupling between the ytterbia selective emitter light pipe and the laser fiber. Based on the preliminary discussion with LLNL and Kigre Inc., it is expected that a Nd SELP first pumping Nd laser and Nd laser pumping an Er:Yb clad laser will provide adequate brightness for a unique laser that can be driven by a combustion source. The Nd laser has lower threshold brightness. The design concept is shown in **Figure 14**.

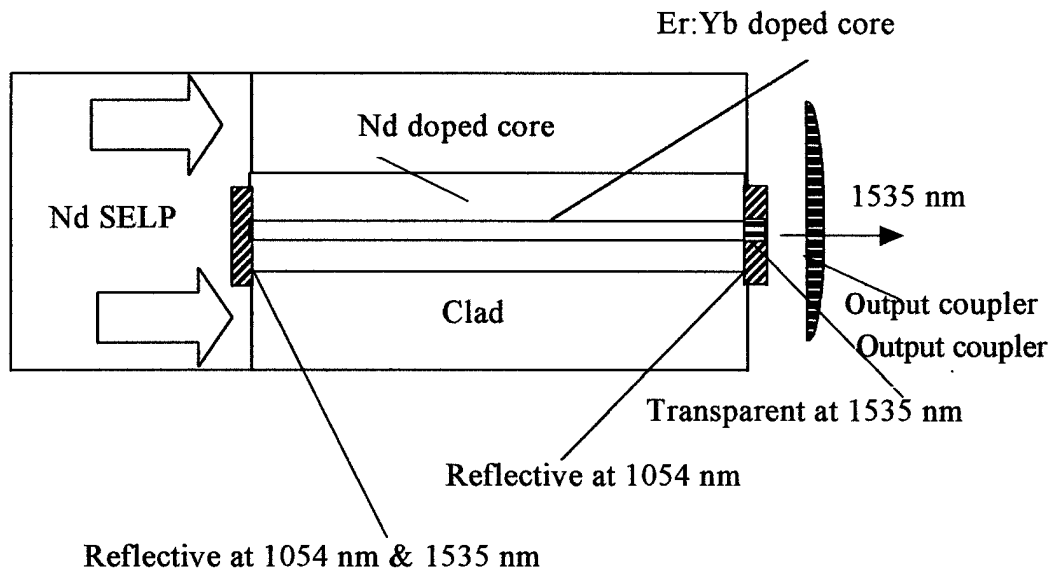


Figure 14. Double core laser eye-safe laser pumping design. SELP first pumps a Nd doped core, which, in turns, pumps Er:Yb eye-safe fiber laser.

6. Bibliography

1. S. Jiang, J. Myers, D. Rhonehouse, R. Belford, and S. Hamlin, "Laser and thermal performance of a new erbium doped phosphate laser glass," SPIE Vol. 2138 (1994).
2. D. E. Pierce and G. Guazzoni, "High temperature optical properties of thermophotovoltaic emitter components," in The Fourth NREL Conference on Thermophotovoltaic Generation of Electricity, T. J. Coutts, J. P. Benner and C. S. Allman Eds. AIP conference Proceeding 460, American Insitute of Physics, Woodbury, N. Y. (1998) pp. 177-196.
3. G. E. Guazzoni and M. F. Rose, "Extended use of photovoltaic solar panels," in The Second NREL Conference on Thermophotovoltaic Generation of Electricity, J. P. Benner, T. J. Coutts and D. S. Ginley Eds. AIP conference Proceeding 358, American Insitute of Physics, Woodbury, N. Y. (1995) pp. 162-176.
4. E. M. Levin, and H. F. McMurdie, Phase Diagrams for Ceramists, M. K. Reser Ed. The American Ceramic Society, Columbus (1975) p.132.
5. N. A. Toropov and V. P. Barzakovskii, High-Temperature Chemistry of Silicates and Other Oxide Systems, (Translated from Russian by C. N. Turton and T.I. Turton), Consultants Bureau, N.Y. (1966) p. 174.